

Infrared spectroscopy of neutral clusters based on a vacuum ultraviolet free electron laser

Cite as: Chin. J. Chem. Phys. **34**, 51 (2021); <https://doi.org/10.1063/1674-0068/cjcp2101018>

Submitted: 29 January 2021 . Accepted: 16 February 2021 . Published Online: 10 March 2021

Gang Li, Chong Wang, Hui-jun Zheng, Tian-tong Wang, Hua Xie, Xue-ming Yang, and Ling Jiang



View Online



Export Citation

Chinese Physical Society



中国物理学会



REVIEW

Infrared Spectroscopy of Neutral Clusters Based on a Vacuum Ultraviolet Free Electron Laser[†]

Gang Li^a, Chong Wang^{a,b}, Hui-jun Zheng^{a,b}, Tian-tong Wang^{a,b}, Hua Xie^a, Xue-ming Yang^{a,c}, Ling Jiang^{a*}

a. State Key Laboratory of Molecular Reaction Dynamics, Collaborative Innovation Center of Chemistry for Energy and Materials, Dalian Institute of Chemical Physics, Chinese Academy of Sciences, Dalian 116023, China

b. University of Chinese Academy of Sciences, Beijing 100049, China

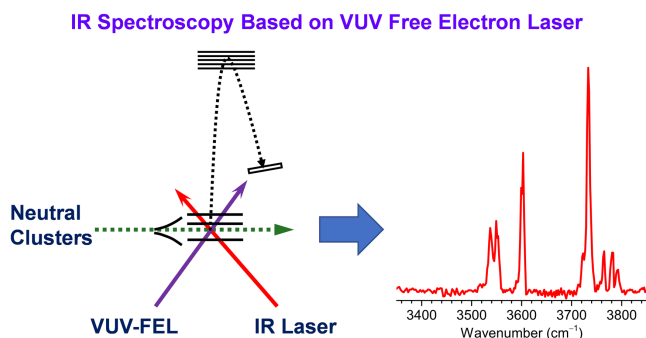
c. Department of Chemistry, School of Science, Southern University of Science and Technology, Shenzhen 518055, China

(Dated: Received on January 29, 2021; Accepted on February 16, 2021)

Spectroscopic characterization of clusters is crucial to understanding the structures and reaction mechanisms at the microscopic level, but it has been proven to be a grand challenge for neutral clusters because the absence of a charge makes it difficult for the size selection and detection. Infrared (IR) spectroscopy based on

threshold photoionization using a tunable vacuum ultraviolet free electron laser (VUV-FEL) has recently been developed in the lab. The IR-VUV depletion and IR+VUV enhancement spectroscopic techniques open new avenues for size-selected IR spectroscopies of a large variety of neutral clusters without confinement (*i.e.*, an ultraviolet chromophore, a messenger tag, or a host matrix). The spectroscopic principles have been demonstrated by investigations of some neutral water clusters and some metal carbonyls. Here, the spectroscopic principles and their applications for neutral clusters are reviewed.

Key words: Clusters, Infrared spectroscopy, Vacuum ultraviolet free electron laser, Structures, Reaction mechanisms



I. INTRODUCTION

The clusters are the aggregates of bound atoms or molecules, which exhibit interesting size-dependent physicochemical properties and bridge the gas and condensed phases [1, 2]. For instance, atmospheric clusters are formed through random collisions and rearrange-

ments of pollutant molecules, and the clusters undergo condensational growth in the atmosphere environment to form larger aerosol particles [3]. The stepwise evolution from molecules to aggregates could be traced by probing the properties of clusters. Catalytic reactions are universally recognized to occur at active centers [4]. While it is difficult to characterize the structure and constitution of the active center of a catalyst, the investigation on the reactions of small molecules with size-selected metal atoms/clusters helps uncover the microscopic mechanism of single-site catalysis processes at the molecular level.

[†]Part of special topic of “the New Advanced Experimental Techniques on Chemical Physics”.

*Author to whom correspondence should be addressed. E-mail: ljiang@dicp.ac.cn

The clusters can be classified as ions (anionic and cationic) and neutrals according to the charge involved. Extensive efforts have been made for the study of ionic clusters, for which size selection and detection are easy. However, it is difficult for the size selection and detection of neutral clusters due to the absence of a charge. Several spectroscopic techniques have been developed to explore the structure, dynamics, and reactivity of some neutral clusters, including Fabry-Perot cavity pulsed Fourier transform microwave spectroscopy [5], IR-molecular-beam spectroscopy [6, 7], scattering analysis of cluster beams [8], helium-droplet evaporation spectroscopy [9], far-IR spectroscopy [10], population-modulated attachment spectroscopy [11], and broadband chirped-pulse Fourier transform microwave spectroscopy [12]. The applications of these optical methods are practically limited to small-sized clusters due to lack of the intrinsic size selectivity. Size-selective infrared spectroscopy of neutral clusters is available achieved by infrared-ultraviolet (IR-UV) double resonance spectroscopy [13], in which the cluster is required to have a chromophore or intermediated state in the UV or visible region for electronic transition measurements to detect the population transfer. This prerequisite thus restricts the widespread application of this technique.

Infrared-vacuum ultraviolet (IR-VUV) spectroscopy, a variant of IR-UV spectroscopy, is an alternative technique for spectroscopic investigation of neutral clusters [14–16], in which VUV threshold photoionization does not require a UV chromophore (intermediate state) and the neutral cluster can be softly ionized without extensive fragmentation. While the ionization energies of neutral clusters span a broad VUV region, the lack of a tunable intense VUV light source precludes the wide application of present IR-VUV spectroscopic technique. Recently, a tunable vacuum ultraviolet free electron laser (VUV-FEL) (50–150 nm) has been developed [17], which makes it possible to measure the size-selected IR spectra of confinement-free, neutral clusters by the IR-VUV scheme, with vibrational modes excited by an IR laser and size-selective detections achieved by VUV soft ionization near the threshold.

Recently, we have developed IR spectroscopy based on threshold photoionization using a tunable VUV-FEL [18, 19]. We have applied this scheme to neutral water clusters and metal carbonyls [18–21]. Here, we review the optical principles of the IR spectroscopies based on VUV-FEL and our recent applications of these tech-

niques to size-selected neutral clusters.

II. EXPERIMENTAL METHODS

The schematic of VUV-FEL-based IR spectroscopy apparatus is shown in FIG. 1, which mainly consists of four parts: cluster source, reflectron time-of-flight mass spectrometer (TOF-MS), VUV-FEL beam line, and IR laser system.

A. Cluster source

Cluster source is a key component for the generation of neutral clusters. Our apparatus has two cluster sources, a pulsed supersonic expansion cluster source and a laser-vaporization supersonic cluster source (FIG. 1).

As shown in FIG. 1(a), pulsed supersonic expansion cluster source is applied to generate the metal-free neutral molecular clusters. A high-pressure pulsed valve (Even-Lavie valve, EL-7-2011-HT-HRR) is used to produce neutral molecular clusters by supersonic expansions of samples seeded in carrier gas, which is capable of producing a very cold molecular beam [22]. In order to prevent liquid sample condensation, the entire gas inlet and the pulsed valve are always heated during the experiments. The concentration of the sample-carrier gas mixtures and the backing pressure are optimized to meet the experimental requirements for a given cluster.

Laser-vaporization supersonic cluster source is utilized to generate the neutral metal-containing clusters. FIG. 1(b) shows a schematic diagram of the laser-vaporization supersonic cluster source, which is a modified version based on this kind of cluster sources previously reported in the literatures [23–25]. A strong and cold supersonic beam is generated by a high-pressure pulse valve equipped with a trumpet-shaped nozzle with a 250 μm hole. An operating gas pulse width is about 22.5 μs . The carried gas is directly injected to growth channel and passes over the surface of the metal rod. A second harmonic of a 532 nm Nd:YAG laser (Beamtech Optronics, Dawa-200) is used to evaporate the metal sample which moves translationally and rotationally. The diameter and length of the waiting room are 5 mm and 16 mm, respectively, and are adjustable for cluster growth. The diameter of the output orifice is 2 mm and the length of the nozzle is 10 mm. The cluster beam passes through a skimmer (Beam Dynamics, Model 50.8) and enters the reflectron TOF-MS cham-

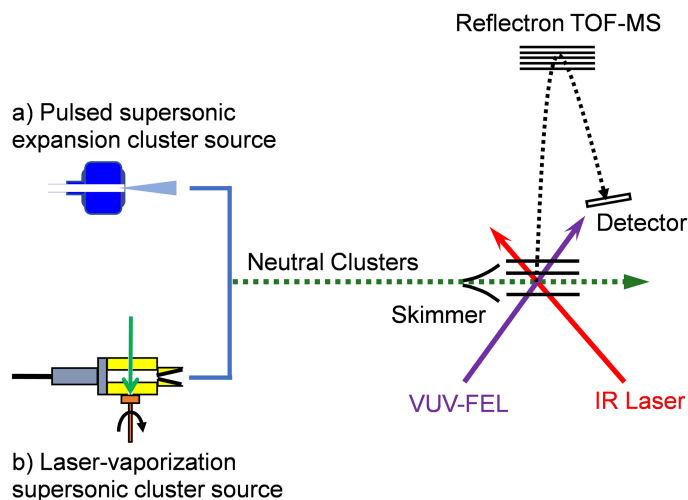


FIG. 1 Schematic diagram of VUV-FEL-based IR spectroscopy apparatus, which is equipped with (a) pulsed supersonic expansion cluster source and (b) laser-vaporization supersonic cluster source.

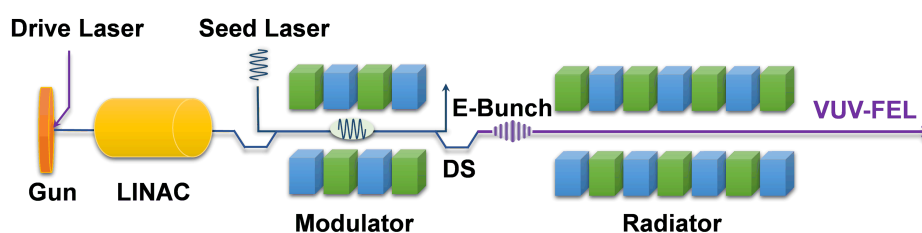


FIG. 2 Schematic of the VUV-FEL beam line.

ber. Charged clusters are deflected out of the molecular beam by the DC electric field of the extraction plates. Our “cutaway” and “offset” type sources can be altered to generate wanted clusters with different compositions, temperatures, and sizes.

B. Reflectron time-of-flight mass spectrometer

The mass spectral signals of VUV-FEL photoionized clusters are detected using a classic Wiley-McLaren time-of-flight mass spectrometer with a reflector to eliminate energy aberration. The acceleration plates are powered by a high-voltage direct current (DC) power supply (2950 V). The neutral clusters are ionized by VUV-FEL light in the center of the extraction region of the reflectron TOF-MS. Cationic clusters are extracted out of the molecular beam by the DC electric field of the accelerator. The electric field of the drift tube and the reflector are shielded by a steel cylinder to avoid interfering the flight of cations. The ions are detected by using a dual microchannel plate (MCP) detector. The transient signals from MCP are first amplified by a fast preamplifier (FEMTO, DHPA-100) and then trans-

mitted to a dual 1 GHz multiscaler (FAST ComTec GmbH, P7888-2) for real-time data acquisition. An external delay generator (Stanford Research Systems, DG645) is used to trigger all the timings of lasers and acquisition card. The best resolution of our TOF-MS is up to ~ 20000 .

C. VUV-FEL beam line

The schematic of the VUV-FEL beam line is shown in FIG. 2. The electron bunch is emitted from the gun when the drive laser hits on the surface of gun cathode. Passing through the linear accelerator (LINAC), the electron bunch is accelerated to desired energy and compressed to high peak current. Before lasing in the radiator, the electron bunch suffers from energy modulation enforced by seed laser in the modulator. Subsequently, the energy modulation is turned into density modulation in dispersion section (DS), and microbunching with spacing of seed laser wavelength emerges in the bunch. Finally, the modulated electron bunch enters the radiator and radiates the highly bright and narrow-bandwidth FEL light at high harmonic of seed

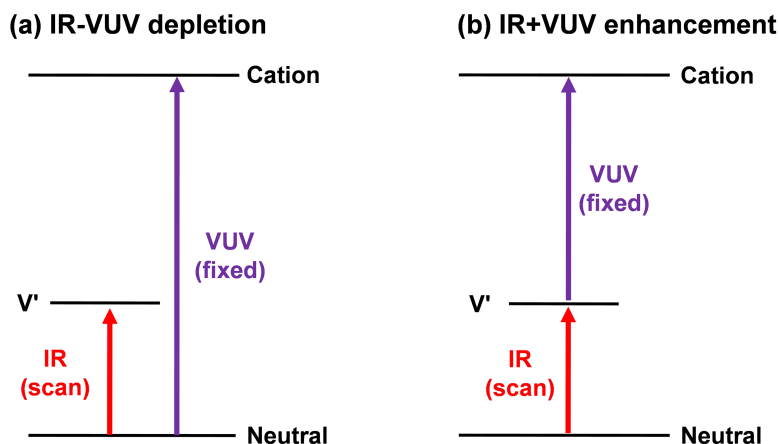


FIG. 3 Excitation schemes of (a) IR-VUV depletion spectroscopy and (b) IR+VUV enhancement spectroscopy.

laser.

The VUV-FEL is operated in high-gain harmonic generation mode [26], in which a seed laser is injected to interact with the electron beam in the modulator. Given the proper optimization of the linear accelerator, a high-quality beam with an emittance as low as ~ 1.5 mm mrad, a projected energy spread of $\sim 1\%$, and a pulse duration of ~ 1.5 ps can be obtained. Generally, the VUV-FEL pulse is operated at 20 Hz, with the maximum operating frequency of 50 Hz. The maximum pulse power of the VUV-FEL light is about $900 \mu\text{J}/\text{pulse}$. Each single VUV-FEL pulse is detected by an online VUV spectrometer for real-time monitoring the spectral characteristics of the pulse.

D. IR laser system

IR laser beam is generated by a potassium titanyl phosphate/potassium titanyl arsenate optical parametric oscillator/amplifier system (OPO/OPA, LaserVision) [27] pumped by an injection-seeded Nd:YAG laser (Continuum Surelite EX). The IR wavelength is tunable from 700 cm^{-1} to 7000 cm^{-1} with a line width of $\sim 1 \text{ cm}^{-1}$. The pulse width of LaserVision system is 7 ns at 10 Hz. The maximum IR pulse energy is $\sim 3 \text{ mJ}/\text{pulse}$ in the region of 700 cm^{-1} to 2000 cm^{-1} and $\sim 30 \text{ mJ}/\text{pulse}$ in the region of $2000\text{--}7000 \text{ cm}^{-1}$. The wavelength of the OPO laser output is calibrated by using a commercial wavelength meter (HighFinesse GmbH, WS6-200 VIS IR).

E. IR-VUV principle and experimental procedure

FIG. 3 shows two kinds of excitation schemes of IR-VUV spectroscopy based on VUV single photon ion-

ization detection, which are used for size-selected vibrational spectroscopic investigation of neutral metal-free molecular clusters and metal-containing complexes. Neutral metal-free molecular clusters are produced by a high-pressure Even-Lavie valve. Species and distribution of these neutral clusters are optimized by fine adjustment of the sample-carrier gas mixtures and the backing pressure. Neutral metal complexes are produced via laser vaporization in expansions of helium seeded with reactant gas using a high-pressure pulsed valve at backing pressures of 3.5–5.0 MPa. The cluster beams pass through a 4 mm skimmer and an aperture into reflectron TOF-MS chamber. Neutral complexes are ionized by a single photon VUV-FEL light and analyzed by Reflectron TOF-MS.

For the IR-VUV depletion spectroscopic study of neutral metal-free molecular clusters, the tunable IR light pulse is introduced at approximately 30–50 ns prior to VUV-FEL pulse in a crossed manner. When the IR laser frequency is resonant with a vibrational transition of a size-selected neutral cluster, vibrational predissociation causes the depletion of VUV ionization signal of neutral cluster. The IR spectrum of this size-selected neutral cluster is recorded by monitoring the depletion of the signal intensity for a specific cluster as a function of IR wavelength (FIG. 3(a)). Since the binding energies of metal-containing complexes are larger than those of metal-free molecular clusters [28–31], IR-induced predissociation is more difficult for metal complexes. The heating of metal complexes via the resonant absorption of infrared photons can enhance ionization efficiency when its ionization potential is just above the VUV photon energy. Then, the IR+VUV enhancement

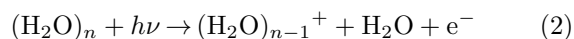
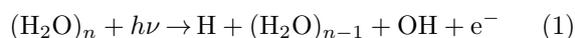
spectrum of a size-selected neutral metal complex can be recorded by monitoring the enhancement in signal intensity as a function of IR wavelength (FIG. 3(b)).

The operating frequencies of the pulsed valve, vaporization laser, and the VUV-FEL are 20 Hz, while that of the IR laser is 10 Hz. The IR spectrum is obtained in the difference mode of operation (IR laser ON minus IR laser OFF). The IR spectrum is determined by converting the measured relative enhancement of the mass spectrometric ion signal ($I(\nu)/I_0$) upon irradiation with IR light to relative absorption cross sections $\sigma(\nu)$ using $\sigma(\nu)=\ln[I(\nu)/I_0]/P(\nu)$. The normalization with the IR laser pulse energy $P(\nu)$ accounts for the variations of $P(\nu)$ over the tuning range. Typical spectra are recorded by scanning the IR laser in steps of 2 cm^{-1} and averaging about 900 laser shots at each spectrum.

III. IR-VUV DEPLETION SPECTROSCOPY OF NEUTRAL WATER CLUSTERS

Water and its interactions with other species are essential in human life. The water clusters play an important role in scientific disciplines ranging from geology to astronomy to biology [32–43]. Spectroscopic investigation of gas-phase water clusters and its transition to bulk water offers an opportunity to better understand the structures and properties of condensed phase water. As the smallest water cluster, the water dimer is a model system for the study of the cooperative hydrogen bond (HB) in liquid water [6, 7, 32, 44–47], which has proven to be difficult to adequately capture through bulk experiments [48].

Dissociative photoionization of neutral water clusters may occur via the “OH loss channel” (reaction (1)) or the “water loss channel” (reaction (2)).



For example, dissociation of the $(\text{H}_2\text{O})_2^+$ ground state into the OH and water loss channels requires dissociation energies of 1.25 and 2.34 eV, respectively [49]. The OH loss channel is energetically favorable and will dominate for cold parent dimers and low (near threshold) ionization energies; dissociation into the water loss channel may occur for higher excitation energies [49]. The OH loss channel undergoes very fast on the sub-picosecond or femtosecond time scale. Accordingly, the

water loss channel is relatively slower and could be reasonably suspended by reducing the excess energy from the ionization via the fine tune of the wavelength and pulse energy of VUV-FEL.

The mass spectra of water clusters ionized at different VUV-FEL wavelengths are shown in FIG. 4. There are two kinds of water clusters in mass spectra, unprotonated $(\text{H}_2\text{O})_n^+$ and protonated $\text{H}(\text{H}_2\text{O})_n^+$. The unprotonated water clusters $(\text{H}_2\text{O})_n^+$ are mainly from ionization of neutral water cluster [50, 51]. The protonated water clusters $\text{H}(\text{H}_2\text{O})_n^+$ are generated via proton transfer and subsequent OH elimination of unprotonated water clusters (reaction (1)), which is the most thermodynamically and kinetically favorable reaction pathway [51, 52]. Many operating conditions (*i.e.*, the wavelength and power of VUV-FEL, concentration of water/helium mixture, stagnation pressure, pulse width of pulse-valve) are optimized to maximize the signal of the $(\text{H}_2\text{O})_2^+$ cluster and avoid the interference from larger clusters. At 98.10 nm (12.64 eV), the unprotonated $(\text{H}_2\text{O})_2^+$ cluster is clearly identified (FIG. 4(a)). The mass spectral signal of $(\text{H}_2\text{O})_3^+$ is detected at 108.00 nm (11.48 eV) (FIG. 4(b)) and appreciably enhanced with wavelength up to 110.00 nm (11.27 eV) (FIG. 4(c)). Therefore, IR spectra of size-selected neutral water dimer are obtained by recording the mass spectral intensities of the unprotonated $(\text{H}_2\text{O})_2^+$ cations at 98.10 nm (FIG. 5). IR-VUV scheme of neutral $(\text{H}_2\text{O})_2$ is free from spectral contamination because the IR excited water clusters dominantly dissociate into the monomer and protonated cluster cation mass channels in the VUV photoionization process as analyzed above [53]. It is a special feature of our method, especially because these neutral clusters are confinement free from the messenger tagging or helium droplets.

As shown in FIG. 5, the experimental IR-VUV depletion spectrum of neutral water dimer consists of four groups of bands (labeled as A–D). Band A is assigned to the antisymmetric OH stretch of the proton acceptor, which are rotationally resolved at 3764, 3780, and 3792 cm^{-1} . Band B at 3732 cm^{-1} comes from the free OH stretch of the proton donor, which is the strongest peak in the IR spectrum. Band C at 3603 cm^{-1} is due to the symmetric OH stretch of the proton acceptor. The splitting of band D is observed at 3537 and 3549 cm^{-1} , which is attributed to the hydrogen-bonded OH stretch of the proton donor. These assignments are

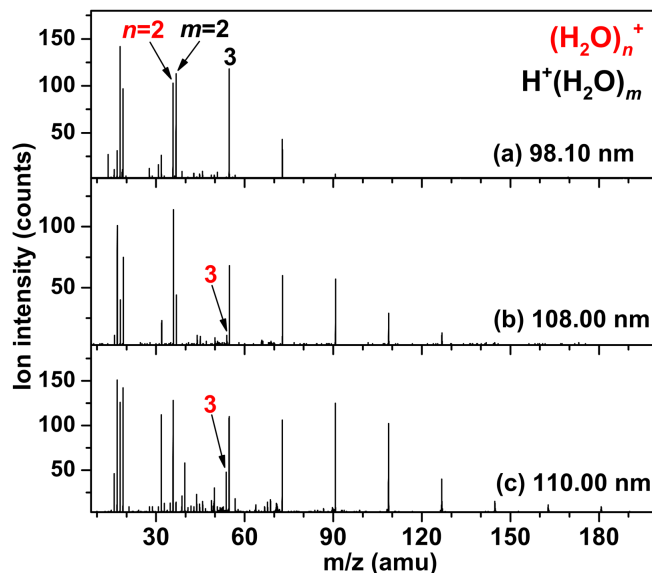


FIG. 4 Time-of-flight mass spectra of the cations produced from the VUV-FEL single-photon ionization process. (a) $\lambda_{\text{VUV-FEL}}=98.10$ nm, (b) $\lambda_{\text{VUV-FEL}}=108.00$ nm, (c) $\lambda_{\text{VUV-FEL}}=110.00$ nm.

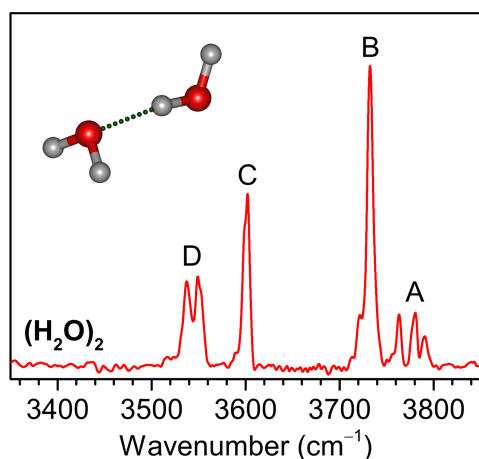


FIG. 5 Experimental IR-VUV depletion spectrum of $(\text{H}_2\text{O})_2$. The OH stretch fundamentals assigned to anti-symmetric OH stretch of the proton acceptor (A), free OH stretch of the proton donor (B), symmetric OH stretch of the proton acceptor (C), and hydrogen-bonded OH stretch of the proton donor (D) are labeled. The inset shows the molecular structure.

supported by quantum mechanical calculations at the MP2/aug-cc-pVTZ and CCSD(T)/aug-cc-pVTZ levels with harmonic approximation and on a 12-dimensional *ab initio* potential energy surface [18].

For the water trimer $(\text{H}_2\text{O})_3$, the vertical ionization energy and dissociation energy for the loss of one water molecule was experimentally measured to be 11.15 eV and 0.84 eV, respectively [51]. The threshold for the water loss channel is estimated to be 11.99 eV, which is

consistent with the calculated value of 11.988 eV [54]. The 3537 and 3549 cm^{-1} bands in our IR spectrum of $(\text{H}_2\text{O})_2$ measured at 98.10 nm (12.64 eV) do not appear in the IR spectrum of $(\text{H}_2\text{O})_3$ measured at 110.00 nm (11.27 eV) [20], indicating that a 98.10 nm (12.64 eV) photon energy might be not large enough for the water loss channel of $(\text{H}_2\text{O})_3$.

The main features in the spectrum are consistent with those in the previous studies [7, 32, 55, 56], especially the size-specific IR-UV spectra of benzene- $(\text{H}_2\text{O})_2$ cluster [32]. In contrast with the general concert in the studies of Huang, Pribble, Page, and Coker *et al.* [7, 32, 55, 56], the major concern raised by Huisken *et al.* was that the ~ 3600 cm^{-1} band was proposed to hydrogen-bonded OH stretch of proton donor and the ~ 3540 cm^{-1} band was presumed to originate from a water trimer [45]. This contradiction could be rationalized by the un-controllable fragmentation caused by the electron impact ionization scheme [45, 57, 58]. In our approach, the soft near-threshold ionization of confinement-free water dimer avoids the extensive fragmentation and the complicatedness of ultraviolet chromophore tagging.

IV. IR+VUV ENHANCEMENT SPECTROSCOPY OF NEUTRAL METAL CARBONYLS

Metal carbonyls are of considerable importance in many heterogeneous and homogeneous catalytic processes such as Fischer-Tropsch chemistry, hydroformy-

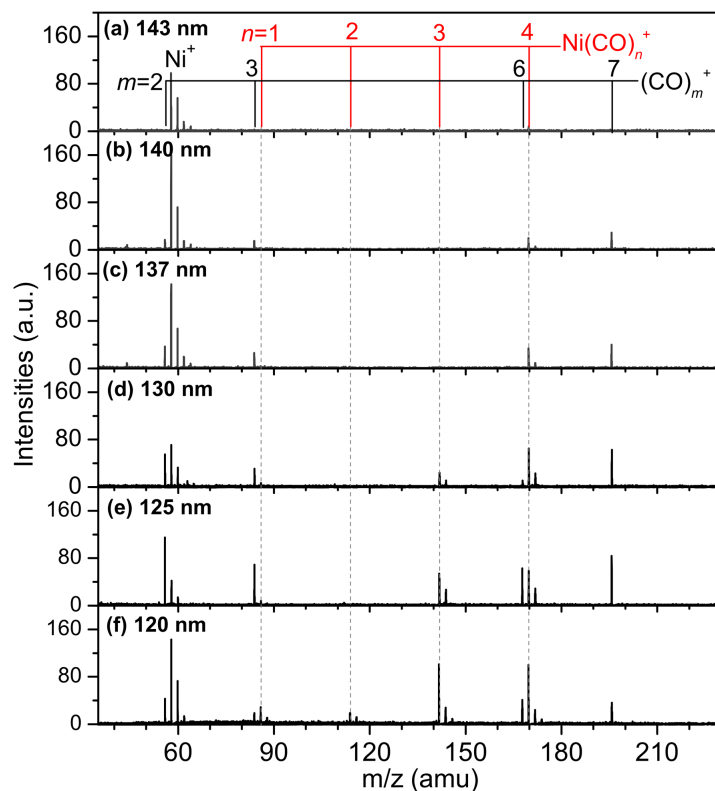


FIG. 6 Time-of-flight mass spectra of the cations produced from the VUV-FEL single-photon ionization process at different VUV-FEL wavelengths: (a) 143.00 nm, (b) 140.00 nm, (c) 137.00 nm, (d) 130.00 nm, (e) 125.00 nm, and (f) 120.00 nm. The scale of mass spectral intensity for each VUV-FEL wavelength is the same.

lation, alcohol synthesis, and acetic acid synthesis [59–61]. Laser vaporization in conjunction with supersonic expansion has been proven to be a very powerful method to produce metal complexes for spectroscopic studies in the gas phase. The combined mass spectrometric techniques with laser-based spectroscopy are among the most direct and generally applicable experimental approaches to obtain vibrational and electronic spectra of metal-containing cluster ions in the gas phase. These methods have been successfully utilized in producing and exploring homoleptic metal carbonyl cations and anions in the gas phase, which serve as typical models for demonstrating the metal-ligand bonding and the electron counting rules. In contrast, vibrational spectroscopic studies of neutral metal carbonyl clusters are rare. Nickel tetracarbonyl, $\text{Ni}(\text{CO})_4$, which was the first metal carbonyl to be discovered in 1890 [62], has been studied by Fourier-transform IR (FT-IR) spectroscopy [63], by matrix isolation spectroscopy [64–67], and theoretical calculations [68–70]. However, the IR spectroscopy of mass-selected $\text{Ni}(\text{CO})_4$ has not been reported. In this section, neutral $\text{Ni}(\text{CO})_4$ is se-

lected as a prototype to demonstrate the performance of IR+VUV enhancement spectroscopic method based on VUV-FEL.

As shown in FIG. 6, the mass spectra of nickel carbonyl clusters ionized by VUV-FEL mainly consist of two groups of peaks: $\text{Ni}(\text{CO})_n^+$ ($n=0-4$) and $(\text{CO})_m^+$ ($m=2-7$). At 143 nm, unique mass spectrum peak belongs to Ni^+ cation (FIG. 6(a)). At 140 nm, the $\text{Ni}(\text{CO})_4^+$ cation and $(\text{CO})_m^+$ ($m=2, 3, 6, 7$) cations are first observed (FIG. 6(b)) and the intensities are significantly enhanced at 137 nm (FIG. 6(c)). As the wavelength of VUV-FEL shortens, the mass spectral signals of $\text{Ni}(\text{CO})_3^+$ and $\text{Ni}(\text{CO})_{1,2}^+$ begin to appear at 130 nm and 120 nm, respectively (FIG. 6 (d, f)). Thus, the mass signal of a size-specific $\text{Ni}(\text{CO})_n$ carbonyl at a selected VUV-FEL wavelength is not interfered by smaller and larger clusters. This allows the densities of size-specific nickel carbonyls to be probed by carefully optimizing the operating conditions (*i.e.*, the wavelength and energy of VUV-FEL, stagnation pressure and concentration of CO carrier gas, and every timing).

The ionization potentials of $\text{Ni}(\text{CO})_{1-4}^+$ have been

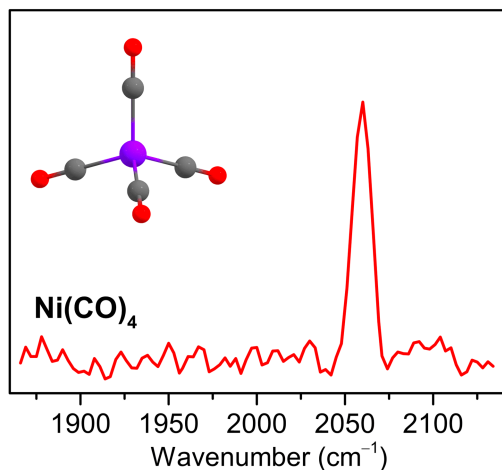


FIG. 7 Experimental IR+VUV enhancement spectrum of $\text{Ni}(\text{CO})_4$. The inset shows the molecular structure.

extensively studied [71–76]. The photoionization data are briefly compared with the mass spectra recorded in this study. Previous studies show the ionization potentials of $\text{Ni}(\text{CO})_4^+$, $\text{Ni}(\text{CO})_3^+$, $\text{Ni}(\text{CO})_2^+$, and $\text{Ni}(\text{CO})^+$ were 8.32 eV (149.01 nm), 8.77 eV (141.37 nm), 10.10 eV (122.75 nm), and 11.65 eV (106.42 nm) [71], respectively. The bonding energy of $\text{OC-Ni}(\text{CO})_3^+$ was 1.36 eV. Therefore, the appearance of $\text{Ni}(\text{CO})_3^+$ ion originating from the decomposition of $\text{Ni}(\text{CO})_4^+$ is thus estimated at $\lambda_{\text{VUV-FEL}} \leq 128.00$ nm (9.68 eV) when $\text{Ni}(\text{CO})_4$ is exposed to VUV ionizing radiation. As shown in FIG. 6(d), the $\text{Ni}(\text{CO})_3^+$ is observed at 130.00 nm, indicating that the signal of $\text{Ni}(\text{CO})_3^+$ is generated from single-photon ionization of neutral $\text{Ni}(\text{CO})_3$ rather than the dissociation of $\text{Ni}(\text{CO})_4^+$. The neutral $\text{Ni}(\text{CO})$ and $\text{Ni}(\text{CO})_2$ cannot be ionized below 125.00 nm, which is consistent with previous photoionization data. These experimental results show the tunable VUV-FE is able to accomplish size-selected ionization of neutral clusters.

With the wavelength of VUV-FEL fixed at 143.00 nm, the IR spectrum of $\text{Ni}(\text{CO})_4$ is recorded from the enhancement in the intensity of $\text{Ni}(\text{CO})_4^+$ mass channel. The intensity of $\text{Ni}(\text{CO})_4$ is linear with IR photon flux by monitoring the IR laser power dependence. As shown in FIG. 7, a single peak is observed at 2060 cm^{-1} in the experimental IR spectrum of $\text{Ni}(\text{CO})_4$, indicative of a high-symmetry structure. Quantum chemical calculations at the B3LYP/def2-TZVPP level predict that $\text{Ni}(\text{CO})_4$ has a Td symmetry structure and the scaled antisymmetric CO stretching vibration of $\text{Ni}(\text{CO})_4$ is 2049 cm^{-1} [19], which is consistent with the

experimental result. The full width at half maximum (FWHM) in the present gas-phase IR spectrum is 11 cm^{-1} . Previously, the IR spectrum of $\text{Ni}(\text{CO})_4$ vapor featured a broad band at 2058 cm^{-1} with a FWHM of 20 cm^{-1} [63]. In matrix isolation experiments, the IR absorption band was found at 2052 cm^{-1} with a FWHM of 3 cm^{-1} in an argon matrix [64–66] and at 2056 cm^{-1} with a FWHM of 4 cm^{-1} in a neon matrix [67]. As compared to the peak positions (2058 and 2060 cm^{-1}) and bandwidths (11 and 20 cm^{-1}) in the gas-phase experiments, the red shifts of the peaks (2052 and 2056 cm^{-1}) and the narrower bandwidths (3 and 4 cm^{-1}) in the matrix isolation experiments are attributed to the interaction of the cold rare-gas matrices with the host molecules [59].

V. CONCLUDING REMARKS

This review summarizes our recent development of infrared spectroscopic techniques based on threshold photoionization detection using a tunable vacuum ultraviolet free electron laser and our applications to some neutral water clusters and some metal carbonyls. As described above, the IR-VUV depletion and IR+VUV enhancement schemes are of quite advantage for IR spectroscopic investigations of neutral clusters without a chromophore, which avoids the extensive fragmentation and the complicatedness of ultraviolet chromophore tagging. Advanced features of IR spectroscopy based on VUV-FEL mainly have three advantages: (i) direct single photon ionization of neutral clusters without confinement (*i.e.*, an ultraviolet chromophore, a messenger tag, or a host matrix); (ii) high sensitivity and size-selectivity by a tunable VUV wavelength and near threshold ionization; (iii) high resolution of IR spectrum for fine structure analysis of neutral clusters. Since the photon energies of VUV-FEL cover the ionization potentials of the vast majority of neutral clusters and their threshold ionization can be readily achieved, the VUV-FEL based IR spectroscopy has the potential to push size-resolved vibrational spectroscopy of neutral clusters to more broad systems, such as atmospheric clusters and the reactions of metal clusters with small molecules (*i.e.*, CO, CO_2 , N_2 , H_2O , NH_3 , CH_4 , C_3H_8 , *etc.*). Along with the advanced theoretical calculations, these studies offer the opportunity for a better understanding of atmospheric new particle formation and rational design of single-atom catalysts with isolated metal atoms dispersed on supports.

VI. ACKNOWLEDGMENTS

We are grateful to many current and former group members for their essential contributions to the development of the VUV-FEL based IR spectroscopies, specifically, Dr. Bing-bing Zhang, Dr. Shu-kang Jiang, and Dr. Zhi Zhao. We thank Prof. Lai-sheng Wang at Brown University for helpful discussions of laser-vaporization supersonic cluster source. We thank outstanding theoretical colleagues, including Prof. Dong-hui Zhang at Dalian Institute of Chemical Physics and Prof. Jun Li at Tsinghua University. The authors gratefully acknowledge the Dalian Coherent Light Source (DCLS) for VUV-FEL beam time and the DCLS staff for support and assistance. This work was supported by the National Natural Science Foundation of China (No.92061203 and No.21688102), the Strategic Priority Research Program of Chinese Academy of Sciences (XDB17000000), International Partnership Program of Chinese Academy of Sciences (121421KYSB20170012), Chinese Academy of Sciences (GJJSTD20190002), K. C. Wong Education Foundation (GJTD-2018-06), and Dalian Institute of Chemical Physics (DICP DCLS201702).

- [1] A. W. Castleman and R. G. Keesee, *Acc. Chem. Res.* **19**, 413 (1986).
- [2] P. E. S. Wormer and A. van der Avoird, *Chem. Rev.* **100**, 4109 (2000).
- [3] R. Zhang, A. Khalizov, L. Wang, M. Hu, and W. Xu, *Chem. Rev.* **112**, 1957 (2012).
- [4] H. S. Taylor, *Proc. Roy. Soc. (London)* **108**, 105 (1925).
- [5] T. J. Balle and W. H. Flygare, *Rev. Sci. Instrum.* **52**, 33 (1981).
- [6] M. F. Vernon, J. M. Lisy, D. J. Krajnovich, A. Tramer, H. S. Kwok, Y. R. Shen, and Y. T. Lee, *Faraday Discuss.* **73**, 387 (1982).
- [7] Z. S. Huang and R. E. Miller, *J. Chem. Phys.* **91**, 6613 (1989).
- [8] U. Buck and H. Meyer, *Phys. Rev. Lett.* **52**, 109 (1984).
- [9] S. Goyal, D. L. Schutt, and G. Scoles, *Phys. Rev. Lett.* **69**, 933 (1992).
- [10] N. Pugliano and R. J. Saykally, *Science* **257**, 1937 (1992).
- [11] E. G. Diken, W. H. Robertson, and M. A. Johnson, *J. Phys. Chem. A* **108**, 64 (2004).
- [12] G. G. Brown, B. C. Dian, K. O. Douglass, S. M. Geyer, S. T. Shipman, and B. H. Pate, *Rev. Sci. Instrum.* **79**, 053103 (2008).
- [13] R. H. Page, Y. R. Shen, and Y. T. Lee, *J. Chem. Phys.* **88**, 4621 (1988).
- [14] H. K. Woo, P. Wang, K. C. Lau, X. Xing, C. Chang, and C. Y. Ng, *J. Chem. Phys.* **119**, 9333 (2003).
- [15] Y. Matsuda, M. Mori, M. Hachiya, A. Fujii, and N. Mikami, *Chem. Phys. Lett.* **422**, 378 (2006).
- [16] H. B. Fu, Y. J. Hu, and E. R. Bernstein, *J. Chem. Phys.* **124**, 024302 (2006).
- [17] D. Normile, *Science* **355**, 235 (2017).
- [18] B. Zhang, Y. Yu, Z. Zhang, Y. Y. Zhang, S. Jiang, Q. Li, S. Yang, H. S. Hu, W. Zhang, D. Dai, G. Wu, J. Li, D. H. Zhang, X. Yang, and L. Jiang, *J. Phys. Chem. Lett.* **11**, 851 (2020).
- [19] G. Li, C. Wang, Q. Li, H. Zheng, T. Wang, Y. Yu, M. Su, D. Yang, L. Shi, J. Yang, Z. He, H. Xie, H. Fan, W. Zhang, D. Dai, G. Wu, X. Yang, and L. Jiang, *Rev. Sci. Instrum.* **91**, 034103 (2020).
- [20] B. Zhang, Y. Yu, Y. Y. Zhang, S. Jiang, Q. Li, H. S. Hu, G. Li, Z. Zhao, C. Wang, H. Xie, W. Zhang, D. Dai, G. Wu, D. H. Zhang, L. Jiang, J. Li, and X. Yang, *Proc. Natl. Acad. Sci. USA* **117**, 15423 (2020).
- [21] G. Li, Y. Y. Zhang, Q. Li, C. Wang, Y. Yu, B. Zhang, H. S. Hu, W. Zhang, D. Dai, G. Wu, D. H. Zhang, J. Li, X. Yang, and L. Jiang, *Nat. Commun.* **11**, 5449 (2020).
- [22] U. Even, J. Jortner, D. Noy, N. Lavie, and C. Cossart-Magos, *J. Chem. Phys.* **112**, 8068 (2000).
- [23] T. G. Dietz, M. A. Duncan, D. E. Powers, and R. E. Smalley, *J. Chem. Phys.* **74**, 6511 (1981).
- [24] L. S. Wang, H. S. Cheng, and J. W. Fan, *J. Chem. Phys.* **102**, 9480 (1995).
- [25] M. A. Duncan, *Rev. Sci. Instrum.* **83**, 041101 (2012).
- [26] L. H. Yu, M. Babzien, I. Ben-Zvi, L. F. DiMauro, A. Doyuran, W. Graves, E. Johnson, S. Krinsky, R. Malone, I. Pogorelsky, J. Skaritka, G. Rakowsky, L. Solomon, X. J. Wang, M. Woodle, V. Yakimenko, S. G. Biedron, J. N. Galayda, E. Gluskin, J. Jagger, V. Sajaev, and I. Vasserman, *Science* **289**, 932 (2000).
- [27] W. R. Bosenberg and D. R. Guyer, *J. Opt. Soc. Am. B* **10**, 1716 (1993).
- [28] K. Muller-Dethlefs and P. Hobza, *Chem. Rev.* **100**, 143 (2000).
- [29] S. R. Gadre, S. D. Yeole, and N. Sahu, *Chem. Rev.* **114**, 12132(2014).
- [30] Z. Luo, A. W. Castleman Jr., and S. N. Khanna, *Chem. Rev.* **116**, 14456 (2016).
- [31] R. H. D. Lyngdoh, H. F. Schaefer III, and R. B. King, *Chem. Rev.* **118**, 11626 (2018).
- [32] R. N. Pribble and T. S. Zwier, *Science* **265**, 75 (1994).
- [33] K. Liu, J. D. Cruzan, and R. J. Saykally, *Science* **271**, 929 (1996).
- [34] K. Nauta and R. E. Miller, *Science* **287**, 293 (2000).
- [35] K. R. Asmis, N. L. Pivonka, G. Santambrogio, M. Brummer, C. Kaposta, D. M. Neumark, and L. Woste,

- Science **299**, 1375 (2003).
- [36] A. E. Bragg, J. R. R. Verlet, A. Kammrath, O. Cheshnovsky, and D. M. Neumark, *Science* **306**, 669 (2004).
- [37] M. Miyazaki, A. Fujii, T. Ebata, and N. Mikami, *Science* **304**, 1134 (2004).
- [38] J. W. Shin, N. I. Hammer, E. G. Diken, M. A. Johnson, R. S. Walters, T. D. Jaeger, M. A. Duncan, R. A. Christie, and K. D. Jordan, *Science* **304**, 1137 (2004).
- [39] R. Bukowski, K. Szalewicz, G. C. Groenenboom, and A. van der Avoird, *Science* **315**, 1249 (2007).
- [40] C. Perez, M. T. Muckle, D. P. Zaleski, N. A. Seifert, B. Temelso, G. C. Shields, Z. Kisiel, and B. H. Pate, *Science* **336**, 897 (2012).
- [41] C. C. Pradzynski, R. M. Forck, T. Zeuch, P. Slavicek, and U. Buck, *Science* **337**, 1529(2012).
- [42] W. T. S. Cole, J. D. Farrell, D. J. Wales, and R. J. Saykally, *Science* **352**, 1194 (2016).
- [43] N. Yang, C. H. Duong, P. J. Kelleher, A. B. McCoy, and M. A. Johnson, *Science* **364**, 275 (2019).
- [44] S. S. Xantheas and T. H. Dunning, *J. Chem. Phys.* **99**, 8774 (1993).
- [45] F. Huisken, M. Kaloudis, and A. Kulcke, *J. Chem. Phys.* **104**, 17 (1996).
- [46] Y. Wang, X. Huang, B. C. Shepler, B. J. Braams, and J. M. Bowman, *J. Chem. Phys.* **134**, 094509 (2011).
- [47] C. Leforestier, K. Szalewicz, and A. van der Avoird, *J. Chem. Phys.* **137**, 014305 (2012).
- [48] D. C. Clary, *Science* **351**, 1267 (2016).
- [49] R. N. Barnett and U. Landman, *J. Phys. Chem.* **99**, 17305 (1995).
- [50] H. Tachikawa, *J. Phys. Chem. A* **108**, 7853 (2004).
- [51] L. Belau, K. R. Wilson, S. R. Leone, and M. Ahmed, *J. Phys. Chem. A* **111**, 10075 (2007).
- [52] B. C. Garrett, D. A. Dixon, D. M. Camaioni, D. M. Chipman, M. A. Johnson, C. D. Jonah, G. A. Kimmel, J. H. Miller, T. N. Rescigno, P. J. Rossky, S. S. Xantheas, S. D. Colson, A. H. Laufer, D. Ray, P. F. Barbara, D. M. Bartels, K. H. Becker, H. Bowen, S. E. Bradforth, I. Carmichael, J. V. Coe, L. R. Corrales, J. P. Cowin, M. Dupuis, K. B. Eisenthal, J. A. Franz, M. S. Gutowski, K. D. Jordan, B. D. Kay, J. A. LaVerne, S. V. Lymar, T. E. Madey, C. W. McCurdy, D. Meisel, S. Mukamel, A. R. Nilsson, T. M. Orlando, N. G. Petrik, S. M. Pimblott, J. R. Rustad, G. K. Schenter, S. J. Singer, A. Tokmakoff, L. S. Wang, C. Wittig, and T. S. Zwier, *Chem. Rev.* **105**, 355 (2005).
- [53] Y. Matsuda, N. Mikami, and A. Fujii, *Phys. Chem. Chem. Phys.* **11**, 1279 (2009).
- [54] R. N. Barnett and U. Landman, *J. Phys. Chem. A* **101**, 164 (1997).
- [55] R. H. Page, J. G. Frey, Y. R. Shen, and Y. T. Lee, *Chem. Phys. Lett.* **106**, 373 (1984).
- [56] D. F. Coker, R. E. Miller, and R. O. Watts, *J. Chem. Phys.* **82**, 3554 (1985).
- [57] F. N. Keutsch, J. D. Cruzan, and R. J. Saykally, *Chem. Rev.* **103**, 2533 (2003).
- [58] A. Mukhopadhyay, W. T. S. Cole, and R. J. Saykally, *Chem. Phys. Lett.* **633**, 13 (2015).
- [59] M. F. Zhou, L. Andrews, and C. W. Bauschlicher, *Chem. Rev.* **101**, 1931 (2001).
- [60] H. J. Freund, G. Meijer, M. Scheffler, R. Schlogl, and M. Wolf, *Angew. Chem. Int. Ed.* **50**, 10064 (2011).
- [61] A. Fielicke, P. Gruene, G. Meijer, and D. M. Rayner, *Surf. Sci.* **603**, 1427 (2009).
- [62] L. Mond, C. Langer, and F. Quincke, *J. Chem. Soc.* **57**, 749 (1890).
- [63] L. H. Jones, R. S. McDowell, and M. Goldblatt, *J. Chem. Phys.* **48**, 2663 (1968).
- [64] R. L. Dekock, *Inorg. Chem.* **10**, 1205 (1971).
- [65] E. P. Kundig, D. McIntosh, M. Moskovits, and G. A. Ozin, *J. Am. Chem. Soc.* **95**, 7234 (1973).
- [66] M. F. Zhou and L. Andrews, *J. Am. Chem. Soc.* **120**, 11499 (1998).
- [67] B. Y. Liang, M. F. Zhon, and L. Andrews, *J. Phys. Chem. A* **104**, 3905 (2000).
- [68] I. A. Howard, G. W. Pratt, K. H. Johnson, and G. Dresselhaus, *J. Chem. Phys.* **74**, 3415 (1981).
- [69] M. R. A. Blomberg, P. E. M. Siegbahn, T. J. Lee, A. P. Rendell, and J. E. Rice, *J. Chem. Phys.* **95**, 5898 (1991).
- [70] J. Li, G. Schreckenbach, and T. Ziegler, *J. Am. Chem. Soc.* **117**, 486 (1995).
- [71] G. Distefano, *J. Res. Natl. Bur. Stand. Sect. A* **74A**, 233 (1970).
- [72] F. I. Vilesov and B. L. Kurbatov, *Dokl. Akad. Nauk. SSSR* **140**, 1364 (1961).
- [73] R. E. Winters and R. W. Kiser, *Inorg. Chem.* **3**, 699 (1964).
- [74] D. R. Bidinosti and N. S. McIntyre, *Can. J. Chem.* **45**, 641 (1967).
- [75] D. R. Lloyd and E. W. Schlag, *Inorg. Chem.* **8**, 2544 (1969).
- [76] S. M. Schildcrout, G. A. Pressley, and F. E. Stafford, *J. Am. Chem. Soc.* **89**, 1617 (1967).